Chiral symmetry restoration at finite temperature and chemical potential in the improved ladder approximation

Yusuke Taniguchi* and Yuhsuke Yoshida†
Department of Physics, Kyoto University, Kyoto 606-01, Japan
(Received 22 December 1995)

The chiral symmetry of QCD is studied at finite temperature and chemical potential using the Schwinger-Dyson equation in the improved ladder approximation. We calculate three order parameters: the vacuum expectation value of the quark bilinear operator, the pion decay constant, and the quark mass gap. We have a second order phase transition at the temperature $T_c = 169$ MeV along the zero chemical potential line, and a first order phase transition at the chemical potential $\mu_c = 598$ MeV along the zero temperature line. We also calculate the critical exponents of the three order parameters. [S0556-2821(97)03004-X]

PACS number(s): 11.10.Wx, 11.15.Tk, 11.30.Rd, 12.38.Cy

I. INTRODUCTION

Chiral symmetry in QCD is dynamically broken at zero temperature. This feature is confirmed by the fact that the pion is the Nambu-Goldstone boson accompanied by this symmetry breaking. On the other hand, it is shown that spontaneously broken symmetries restore at sufficiently high temperature (and/or chemical potential) in some simple models [1]. Then, the same restoration is also expected to hold for dynamically broken chiral symmetry in QCD. This phenomenon is widely believed to be seen in heavy-ion collisions, the early universe, and neutron stars.

There are various attempts to study the phase diagram and critical behavior. In order to do them we need any nonperturbative treatment such as an ε or $1/N$ expansion, lattice simulation, the Schwinger-Dyson equation, and so on. Based on universality arguments it is expected that the critical phenomena of finite temperature QCD are described by a three-dimensional linear σ model with the same global symmetry, in which the ε expansion is used [2]. Lattice simulations are powerful tools to study QCD at finite temperature [3–6]. The Schwinger-Dyson equation in the improved ladder approximation is solved with further approximations and gives dynamical symmetry restoration [7–11]. Nambu–Jona-Lasinio models, as phenomenological models of QCD, provide us with useful pictures about dynamical chiral symmetry breaking and its restoration [12–14]. In these three approaches it is indicated that there is a second order phase transition at $(T,\mu)=(T_c,0)$ and a first order one at $(T,\mu)=(0,\mu_c)$ in the case of the two massless flavors. The phase transition points are found to be of order $T_c \sim 200$ MeV, $\mu_c \sim 400$ MeV.

In this paper we use the Schwinger-Dyson equation in the improved ladder approximation. The advantages of this approach are that it is a convenient tool to study the nature of chiral symmetry, and we easily introduce fermion couplings to the gluon in the chiral limit at finite temperature and chemical potential. Further, we have no degrees of freedom (parameters) to fit the physical observables, and we obtain a definite answer.

In previous attempts further approximations were introduced in addition to the ladder approximation. Some nonperturbative approximation can violate chiral symmetry, and reliable results cannot be obtained. We would like to obtain results keeping chiral symmetry within the framework of the Schwinger-Dyson equation only in the improved ladder approximation.

We calculate the values of the three order parameters: the quark mass gap, the vacuum expectation value of the quark bilinear operator $\langle\bar{\psi}\psi\rangle$, and the pion decay constant. We have a second order phase transition at $T_c = 169$ MeV along the $\mu = 0$ line and a first order phase transition at $\mu_c = 598$ MeV along the $T = 0$ line. The critical exponents of the above three order parameters are extracted at $(T,\mu)=(T_c,0)$, which shows that our formulation is different from mean field theories.

This paper is organized as follows. In Sec. II, we show basic ingredients to study chiral symmetry restoration using the Schwinger-Dyson equation in the improved ladder approximation. The expressions of the three order parameters are given in terms of the quark mass function. The Pagels-Stokar formula is used to calculate the pion decay constant. In Sec. III we give our numerical results. The Schwinger-Dyson equation is numerically solved using a iteration method. We determine the positions and the orders of phase transitions. We also extract the critical exponents. A summary and discussion are found in Sec. IV.

II. SCHWINGER-DYSON EQUATION AT FINITE TEMPERATURE AND CHEMICAL POTENTIAL

The restoration of spontaneously broken symmetry occurs at finite temperature and chemical potential [1]. The phenomenon is described in terms of the imaginary time formalism in gauge theories [15,16].

In this section we show the basic ingredients for solving the Schwinger-Dyson equation at finite temperature and chemical potential. Then, we study dynamical chiral symmetry breaking and its restoration. In this paper all dimensionful quantities are rescaled by using the $\Lambda_{\rm QCD}$, unless otherwise stated.

*Electronic address: tanigchi@gauge.scphys.kyoto-u.ac.jp
†Electronic address: yoshida@yukawa.kyoto-u.ac.jp

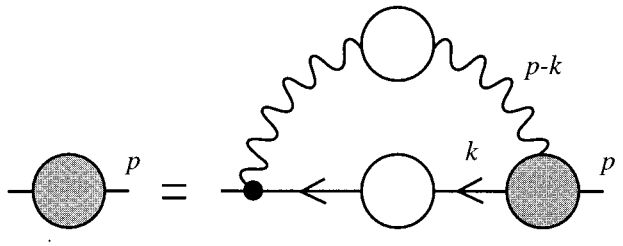

FIG. 1. The Feynman diagram of the Schwinger-Dyson equation. We have the same diagram for the equation at finite temperature and chemical potential.

We consider QCD with massless u and d quarks, and then there is an $SU(2)_L \times SU(2)_R$ chiral symmetry. There are several probes to investigate chiral symmetry such as the quark mass gap, the vacuum expectation value (VEV) of the quark bilinear operator, and the decay constant of the pion. Those are evaluated in terms of the quark mass function $\Sigma(p)$. The mass function is determined by the Schwinger-Dyson equation. We use the improved ladder approximation to solve this equation. We work with the three-flavor β function for the running coupling, since the s quark also contributes to the running of the coupling in the concerned energy range.

At zero temperature this approximation provides us with a convincing result of dynamical chiral symmetry breaking and good values of the lowest-lying meson masses. So we expect that the approximation gives good results even in the case of finite temperature.

To take the effect of finite temperature into account, we work in the imaginary time formalism [15,16]. Let us start with writing down the Schwinger-Dyson equation as in Fig. 1. The diagram is exactly the same as that in zero temperature QCD, since the difference between the usual (zero temperature) field theory and finite temperature field theory stems from the boundary effect of time only. The time components of quark and gluon momenta become discrete. Since quark fields have antiperiodic boundary conditions in the imaginary time direction, we have

$$p^0 = 2\pi i T(n+\tfrac{1}{2}),$$

$$k^0 = 2\pi i T(m+\tfrac{1}{2}), \tag{2.1}$$

where $n, m \in \boldsymbol{Z}$. When the chemical potential μ is introduced, the time component of p in the quark propagator $S_F(p)$ is modified as

$$p_0 \to p_0 - \mu. \tag{2.2}$$

The momentum integration is modified to the summation

$$\int \frac{d^4k}{(2\pi)^4 i} \;\to\; T\sum_{m=-\infty}^{\infty} \int \frac{d^3k}{(2\pi)^3}. \tag{2.3}$$

Then, modifying the Schwinger-Dyson equation at zero temperature according to Eqs. (2.1), (2.2), and (2.3), the Schwinger-Dyson equation at finite temperature is given as

$$\not{p} - S_F(p)^{-1} = T\sum_{m=-\infty}^{\infty} \int \frac{d^3k}{(2\pi)^3} C_2 g^2(p,k) K_{\mu\nu}(p-k) \times \gamma^\mu S_F(k) \gamma^\nu, \tag{2.4}$$

where C_2 is the second Casimir invariant and $-K_{\mu\nu}$ is the gluon tree propagator in the Landau gauge:

$$K_{\mu\nu}(l) = \frac{1}{-l^2}\left(g_{\mu\nu} - \frac{l_\mu l_\nu}{l^2}\right). \tag{2.5}$$

The quantity $g^2(p,k)$ is a one-loop running coupling depending on the momenta p and k. In order to describe a property of QCD we use the following form for the running coupling [17]:

$$g^2(p,k) = \frac{1}{\beta_0} \times \begin{cases} \dfrac{1}{t} & \text{if } t_F < t, \\ \dfrac{1}{t_F} + \dfrac{(t_F - t_C)^2 - (t - t_C)^2}{2t_F^2(t_F - t_C)} & \text{if } t_C < t < t_F, \\ \dfrac{1}{t_F} + \dfrac{(t_F - t_C)}{2t_F^2} & \text{if } t < t_C, \end{cases} \tag{2.6}$$

where $t = \ln(p^2 + k^2)$, $t_C \equiv -2.0$, $\beta_0 = (11N_c - 2N_f)/(48\pi^2)$ is the coefficient of one-loop β function, and t_F is a parameter needed to regularize the divergence of the running coupling at the QCD scale $\Lambda_{\rm QCD}$. We call t_F the infrared regularization parameter. $N_c = 3$ and $N_f = 3$ are the number of colors and flavors, respectively. The running coupling g^2 is smoothly interpolated between the ordinary one-loop running coupling form at $t > t_F$ and a constant value at $t = t_C$. As will be shown, the results do not depend on this particular infrared regularization. It is sufficient to check the t_F dependences only: A change of t_C can be absorbed in that of t_F, and so the infrared behavior of the running coupling is controlled by t_F. By virtue of the running effect of the coupling the resultant mass function, which is determined by Eq. (2.4), reproduces the exact behavior in the high energy region [18]. Notice that this property is needed to preserve chiral symmetry [19].

The quark propagator is expanded by three SO(3)-invariant amplitudes as

$$S_F(p) = \frac{1}{\Sigma(p) + [\mu + B(p)]\gamma^0 - A(p)\not{p}}. \tag{2.7}$$

At the vanishing temperature and chemical potential limits $(T, \mu \to 0)$ the choice of Landau gauge allows us to obtain

$$A(p) = 1,$$

$$B(p) = 0. \tag{2.8}$$

Although we are studying in finite temperature and chemical potential, we assume the relation (2.8) for simplicity. We expect that relation (2.8) is not changed so much in the case of low temperature and chemical potential. As shown later,

the phase transition line of chiral symmetry restoration lies in that region; $T_c, \mu_c \lesssim \Lambda_{\rm QCD}$. Then, the result should not change qualitatively.

Now, substituting Eq. (2.7) into Eq. (2.4) under the condition (2.8), we obtain

$$\Sigma_n(x) = \sum_{m=-\infty}^{\infty} \int y^2 dy K_{nm}(x,y) \times \frac{\Sigma_m(y)}{[2\pi T(m+\frac{1}{2})+i\mu]^2 + y^2 + \Sigma_m(y)^2}, \quad (2.9)$$

where $x = |\mathbf{p}|$ and $y = |\mathbf{k}|$ and

$$K_{nm}(x,y) = \frac{3TC_2 g^2(p,k)}{8\pi^2 xy} \ln\left(\frac{4\pi^2 T^2 (n-m)^2 + (x+y)^2}{4\pi^2 T^2 (n-m)^2 + (x-y)^2}\right). \quad (2.10)$$

Notice that we have the SO(3) rotational invariance but not SO(3,1). The mass function $\Sigma(p)$ is a function of p^0 and $\mathbf{p}^2$, and is rewritten as $\Sigma_n(x)$. In the presence of the chemical potential we easily find from Eq. (2.9) that the mass function takes a complex value satisfying the relation

$$\Sigma_{-n}(x)^* = \Sigma_{n-1}(x) \quad \text{for } n = 1,2,\ldots . \quad (2.11)$$

We solve the Schwinger-Dyson equation (2.9) numerically by an iteration (relaxation) method. The momentum valuables x, y are discretized to be

$$x \rightarrow x_n = \exp\left(\Lambda_{\rm IR} + (\Lambda_{\rm UV} - \Lambda_{\rm IR})\frac{n-1}{N_{\rm SD}-1}\right), \quad (2.12)$$

where $n = 1,2,\ldots,N_{\rm SD}$ and similarly for y. We divide $\ln x$ and $\ln y$ into $N_{\rm SD}$ points. The quantity $\Lambda \equiv \exp(\Lambda_{\rm UV})$ defines the ultraviolet cutoff for the space component of momenta. Therefore an SO(3) symmetric cutoff Λ is introduced, which is needed for numerical calculations. The momentum region of the time component is properly truncated so that the support of the mass function is covered well, as well as that of the space component. We have integrable singularities at $(n,x) = (m,y)$ stemming from the tree level gluon pole, but these should be regularized in the numerical calculation. In order to avoid this singularity we apply a two-point splitting prescription

$$K_{nm}(x,y) \rightarrow \tfrac{1}{2}[K_{nm}(x,y_+) + K_{nm}(x,y_-)], \quad (2.13)$$

with $y_\pm = y\exp[\pm(\Lambda_{\rm UV} - \Lambda_{\rm IR})/(4N_{\rm SD})]$. The validity of this prescription is checked by using the conventional (zero temperature) Schwinger-Dyson equation.

After obtaining the mass function, we immediately evaluate the pion decay constant by using the Pagels-Stokar formula at finite temperature:

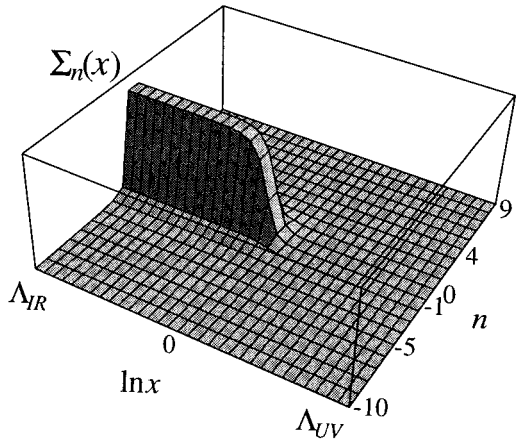

FIG. 2. A typical form of the mass function. We put $(T,\mu) = (90,0)$ MeV. The integer n specifies the time component of the momentum as in Eq. (2.1) and x is given in Eq. (2.12).

$$f_\pi(T,\mu)^2 = \frac{2N_c T}{\pi^2} \sum_n \int_0^\infty x^2 dx \times \frac{\Sigma_n(x)\left(\Sigma_n(x) - \frac{x}{3}\frac{d\Sigma_n(x)}{dx}\right)}{\{[2\pi T(n+\frac{1}{2})+i\mu]^2 + x^2 + \Sigma_n(x)^2\}^2}. \quad (2.14)$$

We also calculate the VEV:

$$\langle \overline{uu} \rangle_\Lambda = \langle \overline{dd} \rangle_\Lambda = \frac{2N_c T}{\pi^2} \sum_n \int_0^\Lambda x^2 dx \times \frac{\Sigma_n(x)}{[2\pi T(n+\frac{1}{2})+i\mu]^2 + x^2 + \Sigma_n(x)^2}. \quad (2.15)$$

The VEV is renormalized at 1 GeV via

$$\langle \overline{\psi\psi} \rangle_{1\ \rm GeV} = \left(\frac{\ln(1\ \rm GeV)}{\ln\Lambda}\right)^{(11N_c - 2N_f)/9C_2} \langle \overline{\psi\psi} \rangle_\Lambda, \quad (2.16)$$

where $\psi = u,d$.

III. NUMERICAL RESULTS

In this section we solve the Schwinger-Dyson equation numerically by an iteration method. We start with an initial form of the mass function and input it in the right-hand side (RHS) of Eq. (2.9). Performing the integration of y and the summation of m, we have an updated form of the mass function, which is taken as a more suitable trial form. After sufficient iterations the functional form converges, giving the true solution with enough accuracy. The convergence of the solution is very rapid off the phase transition regions. A typical form of the mass function is shown in Fig. 2 at $(T,\mu) = (90,0)$ MeV. Let us see the region $\ln x \sim \Lambda_{\rm IR}$ and $n = -10,\ldots,9$. The mass function dumps so fast in the $p_4 \equiv -ip_0$ direction, indicated by n in the figure, that the

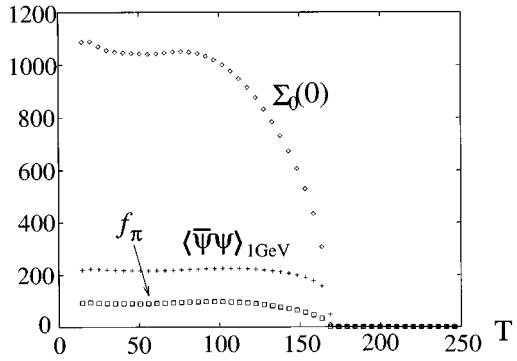

FIG. 3. The functional forms of the order parameters (the mass function, the renormalized VEV, and the pion decay constant) for T along the $\mu=0$ line. The unit is MeV.

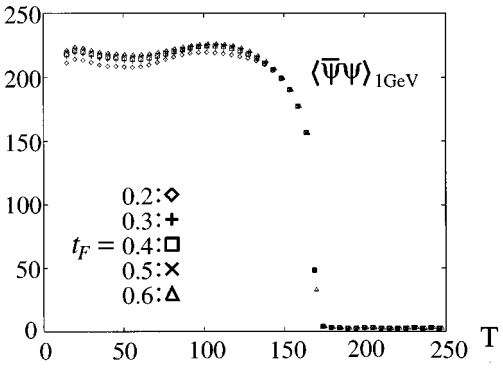

FIG. 4. The t_F dependence of the VEV renormalized at 1 GeV. It changes by 5% at worst against t_F. The unit is MeV.

values of the mass function at $|n|\gtrsim 4$ are much smaller than that at $n=0$ $[\Sigma_{n=4}(x)\sim 10^{-2}\times\Sigma_0(x)]$. The mass function Σ_n begins damping at the Λ_{QCD} scale for increasing $|n|$, which corresponds to $2\pi T(n+1/2)\sim\pm\Lambda_{\mathrm{QCD}}$. At $T=90$ MeV this corresponds to $n+1/2\sim\pm 1.0$. This implies a dimensional reduction at sufficiently high temperature; i.e., four-dimensional theory at finite temperature belongs to the same universality class as that of a three-dimensional theory with the same symmetry.

We use the renormalized VEV and the pion decay constant as order parameters of chiral symmetry. The dynamical mass of the quark itself is also an order parameter.

We determine the value of Λ_{QCD} from the experimental result $f_\pi=93$ MeV at $T=\mu=0$, and we have $\Lambda_{\mathrm{QCD}}=592$ MeV using Eq. (2.14) at $t_F=0.5$. This is our result of Λ_{QCD} obtained by using the one-loop β function. In this paper we put the infrared regularization parameter $t_F=0.5$ and show later that the physical observables as well as the phase transition line do not depend on t_F.

A. Zero chemical potential case

First, we study the phase transition along the $\mu=0$ line. The phase transition point is defined so that three order parameters of the mass gap, $\Sigma_{n=0}(x=0)$, the renormalized VEV $\langle\psi\psi\rangle_{1\,\mathrm{GeV}}$, and the pion decay constant f_π, vanish. We show the temperature dependences of these order parameters in Fig. 3 with two massless flavors. The $\mathrm{SU}(2)_L\times\mathrm{SU}(2)_R$ chiral symmetry restores at $T=T_c=169$ MeV. We have a second order phase transition. We have the same result as that of lattice simulations [5,6] with two flavors in which the phase transition is second order at $T_c\sim 200$ MeV.

The ladder approximation, used here, gives no flavor dependence, since the dependence essentially comes through only the running effect of the coupling, whereas the flavor dependence is suggested by universality arguments [2] and it is confirmed by lattice simulations [3,5,6], where we have a second order phase transition at $N_f=2$ and first order ones at $N_f\geqslant 3$. Nambu–Jona-Lasinio (NJL) models [12–14] imply that the inclusion of the effect of the $\mathrm{U}(1)_A$ anomaly, the so-called the instanton effect, allows us to obtain the same flavor dependence as that in the lattice simulations.

The important point in studying chiral symmetry is that the approximation used should preserve symmetry. Fortunately, the ladder approximation itself is consistent with the chiral symmetry [19]. However, many investigations violate chiral symmetry, where further approximations are used in addition to the ladder [7,9,10]. In order to preserve symmetry the high energy behavior of the quark mass function must be consistent with the result of the operator product expansion (OPE) [19]:

$$\Sigma_n(\mathbf{p}^2)\sim\frac{g^2(x)}{x}(\ln x)^{9C_2/(11N_c-2N_f)}\quad\text{as}\quad x\equiv p_4^2+\mathbf{p}^2\sim\infty. \tag{3.1}$$

Here we should notice that even in the finite temperature case the high energy behavior of the mass function is the same as that of the zero temperature case, since the temperature effect is suppressed in the high energy region. In Refs. [7,9,10] their further approximation ($\Sigma=\mathrm{const}$) does not satisfy Eq. (3.1); on the other hand, in Ref. [11] they adopt an ansatz consistent with Eq. (3.1) up to the logarithmic correction, while our formalism exactly reproduces the OPE result (3.1).

We check the dependence of the order parameters on the infrared regularization parameter t_F. The physical observables $\langle\bar{\psi}\psi\rangle_{1\,\mathrm{GeV}}$ and $f_\pi(T)$ should not depend on the parameter t_F. We confirm this requirement. The dependence of the renormalized VEV $\langle\bar{\psi}\psi\rangle_{1\,\mathrm{GeV}}$ and the pion decay constant $f_\pi(T)$ is shown in Figs. 4 and 5. The values of the renormalized VEV and the f_π change, at worst, by 5% and 8% against $t_F=0.2$–0.6, respectively. These values of $t_F=0.2$–0.6 correspond to those of the running coupling

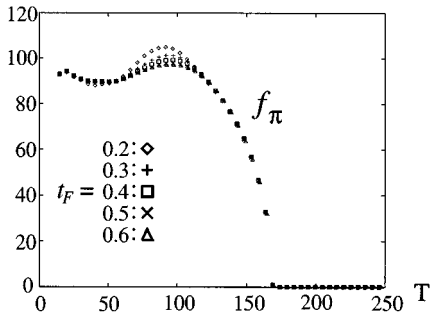

FIG. 5. The t_F dependence of the pion decay constant. It changes by 8% at worst against t_F. The unit is MeV.

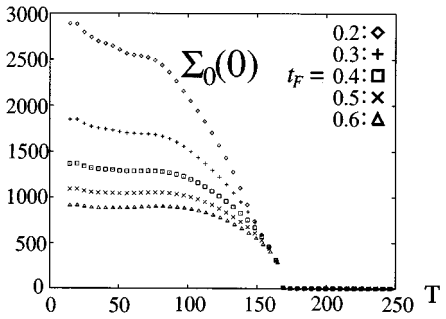

FIG. 6. The t_F dependence of the mass function. We have a strong dependence. The unit is MeV.

$g^2(p=k=0)=570$–92.6. Moreover, the phase transition point is fairly stable against t_F. We conclude that there is no t_F dependence of the physical observables and the position of the phase transition point.

We also show the dependence of the mass function in Fig. 6. We have a strong t_F dependence. Since the mass function is not a physical observable, it may depend on the regularization parameter t_F. However, the phase transition point determined using the mass function is fixed.

Let us examine the critical behavior of the system. Since we have a second order phase transition at $(T,\mu)=(T_c,0)$, the three order parameters behave near the phase transition point as

$$\langle\overline{\psi\psi}\rangle_{1\ \mathrm{GeV}}\sim\left(1-\frac{T}{T_c}\right)^{\beta},$$

$$\Sigma_0(0)\sim\left(1-\frac{T}{T_c}\right)^{\nu},$$

$$f_\pi(T)\sim\left(1-\frac{T}{T_c}\right)^{\beta'}, \tag{3.2}$$

where $T<T_c$. The critical exponents β, ν and β' are numerically extracted by using a χ^2 fitting. The order parameters $\mathcal{O}$ $[=\langle\overline{\psi\psi}\rangle_{1\,\mathrm{GeV}},\Sigma_0(0),f_\pi(T)]$ are fitted by the linear functional form $\ln\mathcal{O}(T)=A+\gamma\ln(1-T/T_c)$, and the fitting

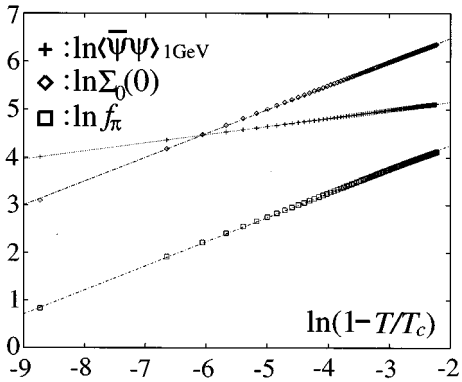

FIG. 7. The χ^2 fittings for extracting the critical exponents of the renormalized VEV, the mass gap, and the pion decay constant. We draw the best fitted lines of the form $A+\gamma\ln(1-T/T_c)$.

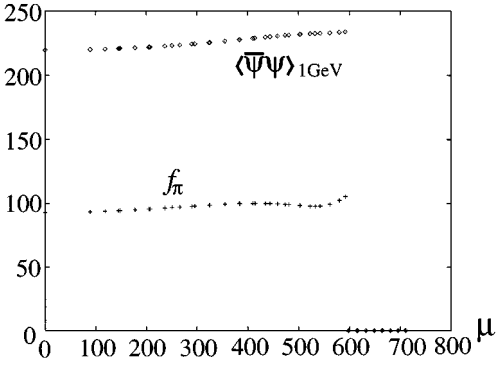

FIG. 8. The functional forms of the renormalized VEV and the pion decay constant for μ along $T=0$ line. The unit is MeV.

parameters are A and γ $(=\beta,\nu,\beta')$ with $T_c=169$ MeV. We have good fittings, which is shown in Fig. 7. The result is

$$\beta=0.171,\quad \nu=0.497,\quad \beta'=0.507. \tag{3.3}$$

These values are different from those in mean field theories. If we consider mean field theories, we would have the relation $\beta=\nu$ since $\Sigma\sim\langle\overline{\psi\psi}\rangle$.

B. Zero temperature case

Next, we study the phase transition along the $T=0$ line. As is seen from Eq. (2.9), the mass function has an imaginary part for $\mu\neq0$. The functional forms for μ are shown of the renormalized VEV $\langle\overline{\psi\psi}\rangle_{1\,\mathrm{GeV}}$, the pion decay constant $f_\pi(\mu)$, and the real and imaginary parts of the mass gap in Figs. 8 and 9. The $\mathrm{SU}(2)_L\times\mathrm{SU}(2)_R$ chiral symmetry restores at $\mu=\mu_c=598$ MeV. We have a strong first order phase transition. Here, we check that the infrared regularization parameter t_F does not affect the physical observables and the nature of the phase transition.

Let us compare our result with those of other approaches. There is no lattice simulation at so large a chemical potential that we can directly see the phase transition. A phase transition is suggested by extrapolating the result of lattice simulations around small μ [4]. On the other hand, there are many attempts using Schwinger-Dyson equations [7,9,11] and NJL models [13,14]. Previous attempts [9,11] in the ladder approximation give a first order phase transition. NJL [13,14] models with the instanton effect also give the same at $N_f=2,3$. Therefore, our result confirms theirs. Our

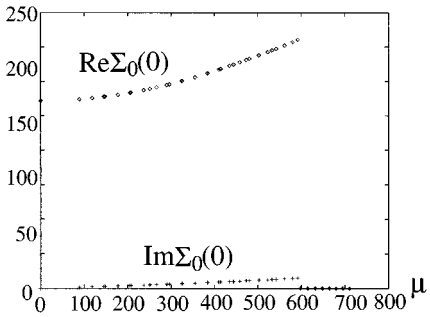

FIG. 9. The functional forms of the real and the imaginary parts of the mass function for μ along $T=0$ line. The unit is MeV.

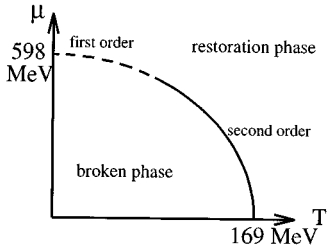

FIG. 10. The schematic view of the phase diagram from our result.

advantage is that we have no parameter which modifies the physical result.

C. Phase diagram

Finally, we study the phase diagram of chiral symmetry restoration. Near the $\mu=0$ line we have second order phase transitions and near the $T=0$ line we have first order ones. In both cases the convergences of updating the mass function are rapid, good for solving the Schwinger-Dyson equation. Unfortunately, near the phase transition line in the middle region, the convergences are too bad to obtain solutions with a suitable accuracy. However, a natural guess will be that the order of phase transitions continuously changes from first order to second order, through weak first order, in the middle region shown as in Fig. 10. This type of diagram is also obtained in Refs. [11,13], which is the same as that of the two-dimensional Gross-Neveu model in Refs. [20,21].

IV. SUMMARY AND DISCUSSION

In this paper have we studied the chiral symmetry restoration at finite temperature and chemical potential in QCD. We use the improved ladder approximation and the imaginary time formalism. The improved ladder approximation does not violate chiral symmetry, since the high energy behavior of the quark mass function is consistent with the result of the operator product expansion [19] even at finite temperature and chemical potential. The phase transition point (or line) is determined by using three order parameters, i.e., the VEV $\langle\psi\psi\rangle_{1\,\mathrm{GeV}}$ renormalized at 1 GeV, the quark mass gap $\Sigma_0(0)$, and the pion decay constant f_π. In the improved ladder approximation the infrared regularization parameter t_F must be introduced as in Eq. (2.6) in order to regularize the running coupling. We, however, observe that physical quantities do not depend on the parameter t_F. Then, our results are obtained without any degrees of freedom other than Λ_{QCD} which is determined by putting $f_\pi=93$ MeV at $(T,\mu)=(0,0)$.

In the case of the vanishing chemical potential $\mu=0$ we have a second order phase transition at $T_c=169$ MeV. The critical exponents are extracted in Eq. (3.3). This shows that QCD in the improved ladder approximation is different from mean field theories. In the case of the vanishing temperature $T=0$ we have a strong first order phase transition at $\mu=598$ MeV.

In the $(T,\mu)=(0,0)$ limit the functional forms $A(p)=1$ and $B(p)=0$ as in Eq. (2.8) give a solution of the Schwinger-Dyson equation in the Landau gauge. In this paper we put these forms for any (T,μ) for simplicity. We should check the validity of this prescription. In the middle region ($0<T<T_c$ and $0<\mu<\mu_c$) near the phase transition line the calculation of the mass function is too difficult for the error to vanish in the iteration method. It is necessary to obtain a more efficient method for solving the Schwinger-Dyson equation in this region. After these problems are settled, the framework of the improved ladder approximation becomes a more convenient tool to figure out the nature of chiral symmetry, since it is easy to introduce fermions in the chiral limit.

ACKNOWLEDGMENTS

We would like to thank T. Hatsuda and Y. Kikukawa for valuable discussions and comments.

[1] D. A. Kirzhnits and A. D. Linde, Phys. Lett. **42B**, 471 (1972); S. Weinberg, Phys. Rev. D **9**, 3357 (1974); L. Dolan and R. Jackiw, *ibid.* **9**, 3320 (1974).

[2] R. D. Pisarski and F. Wilczek, Phys. Rev. D **29**, 338 (1984); K. Rajagopal and F. Wilczek, Nucl. Phys. **B399**, 395 (1993).

[3] J. Polonyi, H. W. Wyld, J. B. Kogut, J. Shigemitsu, and D. K. Sinclair, Phys. Rev. Lett. **53**, 644 (1984); R. Gupta, G. Guralnik, G. W. Kilcup, A. Patel, and S. R. Sharpe, *ibid.* **57**, 2621 (1986); E. V. Kovacs, D. K. Sinclair, and J. B. Kogut, *ibid.* **58**, 751 (1987).

[4] J. Kogut, H. Matsuoka, M. Stone, H. W. Wyld, S. Shenker, J. Shigemitsu, and D. K. Sinclair, Nucl. Phys. **B225**, 93 (1983); J. B. Kogut, M. P. Lombardo, and D. K. Sinclair, Phys. Rev. D **51**, 1282 (1995).

[5] F. R. Brown, F. P. Butler, H. Chen, N. H. Christ, Z. Dong, W. Schaffer, L. I. Unger, and A. Vaccarino, Phys. Rev. Lett. **65**, 2491 (1990).

[6] Y. Iwasaki, K. Kanaya, S. Sakai, and T. Yoshie, in *Lattice '93*, Proceedings of the International Symposium, Dallas, Texas, edited by T. Draper *et al.* [Nucl. Phys. B (Proc. Suppl.) **34**, (1994)].

[7] D. Bailin, J. Cleymans, and M. D. Scadron, Phys. Rev. D **31**, 164 (1985).

[8] A. Kocić, Phys. Rev. D **33**, 1785 (1986).

[9] T. Akiba, Phys. Rev. D **36**, 1905 (1987).

[10] T. S. Evans and R. J. Rivers, Z. Phys. C **40**, 293 (1988).

[11] A. Barducci, R. Casalbuoni, S. De Curtis, R. Gatto, and G. Pettini, Phys. Rev. D **41**, 1610 (1990); Phys. Lett. B **240**, 429 (1990).

[12] T. Hatsuda and Kunihiro, Phys. Rev. Lett. **55,** 158 (1985); Prog. Theor. Phys **74**, 765 (1985); Phys. Lett. B **198**, 126 (1987).

[13] M. Asakawa and K. Yazaki, Nucl. Phys. **A504**, 668 (1989).

[14] M. Lutz, S. Klimt, and W. Wise, Nucl. Phys. **A542**, 521 (1992).
[15] T. Matsubara, Prog. Theor. Phys. **14**, 351 (1955); C. W. Bernard, Phys. Rev. D **9**, 3312 (1974); H. Hata and T. Kugo, *ibid.* **21**, 3333 (1980).
[16] R.P. Feynman and A.R. Hibbs, *Quantum Mechanics and Path Integrals* (McGraw-Hill, New York, 1965); A. L. Fetter and J. D. Walecka, *Quantum Theory of Many-Particle Systems*, (McGraw-Hill, New York, 1971).
[17] K.-I. Aoki, M. Bando, T. Kugo, M. G. Mitchard, and H. Nakatani, Prog. Theor. Phys. **84**, 683 (1990).
[18] H. D. Politzer, Nucl. Phys. **B117**, 397 (1976).
[19] K. Higashijima, Phys. Rev. D **29**, 1228 (1984); V. A. Miransky, Sov. J. Nucl. Phys. **38**, 280 (1984).
[20] U. Wolff, Phys. Lett. **157B**, 303 (1985).
[21] T. Inagaki, T. Kouno, and T. Muta, Int. J. Mod. Phys. A **10**, 2241 (1995).